Asociación Argentina
de Mecánica Computacional

Mecánica Computacional Vol XXVI, pp.1471-1482
Sergio A. Elaskar, Elvio A. Pilotta, Germán A. Torres (Eds.)
Córdoba, Argentina, Octubre 2007

INFLUENCE OF THE IRREVERSIBILITY OF INTERFACE CONSTITUTIVE RELATIONS ON THE PROPAGATION OF FATIGUE CRACKS

Anderson Machado, Eduardo Bittencourt and Inácio B. Morsch

Centro de Mecânica Aplicada e Computacional, Univesidade Federal do Rio Grande do Sul, Avenida Osvaldo Aranha, 99, Porto Alegre, RS, Brazil, bittenco@cpgec.ufrgs.br, http://www.ppgec.ufrgs.br/Cemacom

Keywords: Fatigue, Finite Element, cohesive interface, oxide.

Abstract. Prediction of life in fatigue is still based on purely phenomenological or empiric relations, in most cases in Engineering practice. The Paris' law is one of the few consolidated tools to calculate propagation velocity of fatigue cracks based on Fracture Mechanics, although being also a phenomenological relation.

The cohesive interface method has been used intensively lately as a tool to simulate cracking process in metals with great success. More recently, few attempts to use this method to predict life in fatigue have been done. Such works follow the general idea that during the loading-unloading, cohesive law should present some hysteresis, function of parameters that measure damage during cycling process.

In this work, the cohesive surface method will be used as an attempt to model the rupture in fatigue. However, dissipation during cyclic loading in the present work will not introduce new damage parameters, being a residual opening after unloading the only source of irreversibility. Such hypothesis is based on the fact that oxidation films develop after opening.

The unloading path may have also an important effect on monotonic crack propagation, since local unloading, near the crack tip, are expected.

To simulate propagation, the cohesive surface was implemented in a Element code. Preliminary results for a 7075-T6 aluminum show good data fitting, indicating that the hypothesis is feasible. In the examples analyzed, only Mode I of propagation was considered. Plastic strains on the crack tip were small, indicating the validity of the Linear Elastic Fracture Mechanics. Dynamic and monotonic crack propagation are also considered here, showing that the local unloading near crack tip may have an important effect on the kinematics of the propagation.

1 INTRODUCTION

The propagation process of fatigue cracks can be divided in nucleation, growth and final fracture (stage I, II and III, respectively). Nucleation depends on microscopic defects as the PSBs (Persistent Slip Band) and plastic strains, being then controlled by shear stresses. The crack growth velocity (da/dN; a = crack length, N = number of cycles) is very low in this case or visible only at atomic level. In the growth stage, propagation is a function of the variation of the stress-intensity factor ($\Delta K_I = K_I^{max} - K_I^{min}$), being the velocity da/dN increased substantially in this stage. In this case the propagation occurs according to the Paris' law:

$$\frac{da}{dN} = C(\Delta K_I)^m \tag{1}$$

since few conditions are fulfilled, as the validity of Linear Elastic Fracture Mechanics (LEFM) and application of cyclic loading (no amplitude variation). C e m are material constants. Several theories have been formulated to determine such constants, among them the cohesive interface methodology, which is the focus of this work.

The use the cohesive interface methodology with return to origin during unloading does not lead to fatigue (Andrés et al. 1999 and Nguyen et al. 2000). In this case a plastic shakedown occurs after few cycles and the crack opening stops. Then the methodology will work after some irreversibility on traction/crack opening relation is introduced. Basically, irreversibility can be introduced by two ways: i) considering a residual opening caused, for instance, by oxides as in Deshpande et al. (2002) and ii) using a cohesive law that presents hysteresis as in Nguyen et al. (2000). In the latter case, a phenomenological damage theory must be formulated in order to update fracture parameters as a function of the number of cycles.

The presence and formation of oxides seems to have fundamental importance on the process of crack growing. Indeed, Peloux (1970), suggested that in vacuum, cyclic loading was reversible, or fatigue did not occur. Later on, it became clear that in the absence of oxides, propagation velocity of fatigue cracks was decreased in more than one order of magnitude (see Suresh, 1998). The reason oxides produce such effect is linked to the irreversibility they induce, avoiding that the crack returns to the same opening it had before loading/unloading cycle. According to Do et al. (1997), a layer of oxide up to 6 nm has been predicted for aluminum, on normal atmospheric conditions. However, this value can be increased significantly by the friction between crack surfaces (fretting). For low values of ΔK_I and ratios $R = K_I^{min}/K_I^{max}$, near zero, when the crack faces are too close, Suresh et al (1981) found values of oxide layer in fatigue cracks up to twenty times thicker than the layers developed in new surfaces exposed to the same humidity.

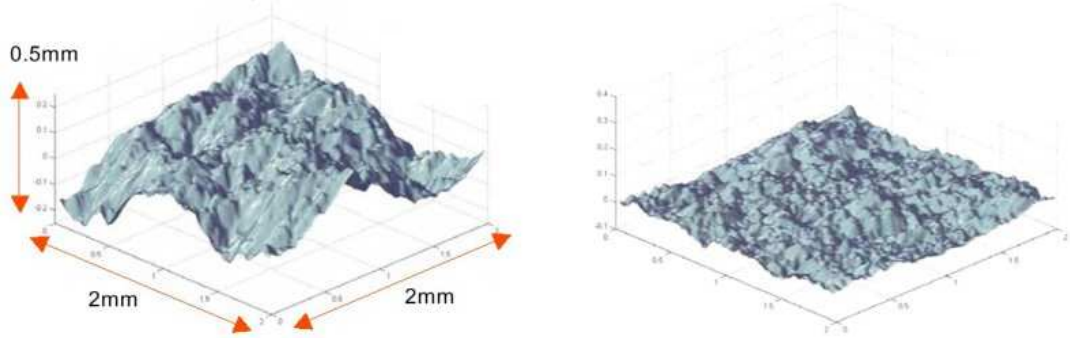

Figure 1: 3D tomography images of fatigue crack surfaces in a 2xxx aluminum series, according to Kamp et al. (2007). Left low ΔK_I, right high ΔK_I

On the other side, a significant superficial roughness can be found in fatigue crack surfaces, as shown in Figure 1 (see Kamp et al., 2007), even for high values of ΔK_I. Due to roughness, crack surface friction and then the enhanced development of oxides due to fretting may occur in the whole fatigue process, although less pronounced at large ΔK_I.

To consider a cyclic degradation of cohesive surface stiffness and peak traction is the other way of introducing fatigue using the cohesive interface methodology. Examples of such methodologies can be find in the works of Ural et al. (2007), Nguyen et al. (2000), Roe and Sigmund (2003), etc. These methodologies need the definition of new state variables, to be determined experimentally, besides the ones used in the monotonic fracture model.

The aim of the present work is to explore the cohesive interface methodology using the first hypothesis (oxide formation), verifying the range of ΔK_I and R it gives results compatible with experiments. Also, Paris' constants will be calculated based on numerical results. The material used will be a 7xxx aluminum series. The effect of unloading will be also investigated in a fracture case where monotonic loading is applied. In this case a PMMA plate subjected to dynamic loading is investigated. In item 2 is presented the cohesive interface methodology; in item 3 is described the implementation in a finite element context. In item 4, applications to cyclic and monotonic loading are studied, being final remarks made in item 5.

2 COHESIVE INTERFACE METHODOLOGY

The fracture behavior is here analyzed using the Finite Element Method (FEM) with cohesive elements placed between FEs (as in Xu and Needleman, 1994). Constitutive equations need to be defined for cohesive elements. Then for an interface opening $\{\Delta\}$ in a 2-D domain, traction $\{T\}$, a normal vector $\{n\}$ and a tangent vector $\{t\}$ to the interface, it can be defined that:

$$\begin{matrix} \Delta_n = \{\Delta\}.\{n\} \\ T_n = \{T\}.\{n\} \end{matrix} \quad \text{and} \quad \begin{matrix} \Delta_t = \{\Delta\}.\{t\} \\ T_t = \{T\}.\{t\} \end{matrix}. \tag{2}$$

A normal cohesive traction relates to normal opening according to the phenomenological relation below (considering null tangential opening):

$$T_n = -\frac{\phi_n \Delta_n}{\delta_n^2} \exp\left(-\frac{\Delta_n}{\delta_n}\right) \tag{3}$$

Equation (3) has a peak value (σ_{max}) for a normal opening $\Delta_n = \delta_n$; ϕ_n is the fracture energy for Mode I of propagation. The dissipated energy during the crack opening is obtained integrating (3) in Δ_n (or the area under the curve T_n x Δ_n) . For $\Delta_n >> \delta_n$., the area is equal to fracture energy ϕ_n and the cohesive traction T_n is zero, which indicates fracture of the interface. σ_{max} is around 3 x σ_y where σ_y is the yielding stress, for metals. For fragile materials, σ_{max} is around E/10 where E is the longitudinal elastic modulus.

Deshpande et al. (2002) proposed an irreversible cohesive law where, in the case of unloading after the peak stress, the relation followed is no longer exponential, becoming linear and with a residual opening for null traction, according to Figure 2. This occurs due to oxide formation after crack/interface opening. Then, if the interface is loaded monotonically until an opening Δ^a_{nmax}, the relation T_n *x* Δ_n followed is exponential. If at this point occurs an unloading, the return will not occur by the exponential relation, but by the linear law, according to Figure 2. The result is a residual opening for null traction, which gives an irreversibility in the cycle that may lead to fatigue. For a new loading, the relation followed is

linear until Δ^{a}_{nmax} is reached, when again the exponential curve is obeyed, until a new unloading point (Δ^{b}_{nmax}) is achieved. The relation that defines traction during unloading is given by equation (4):

$$T_n = -\alpha \frac{e\,\sigma_{max}}{\delta_n} \Delta_n \tag{4}$$

where α is a factor that here will be changed from 0,1 to 20, which corresponds to consider different levels of residual openings or different layer thickness of oxides (in Deshpande et al. 2002 α is constant and equal to one).

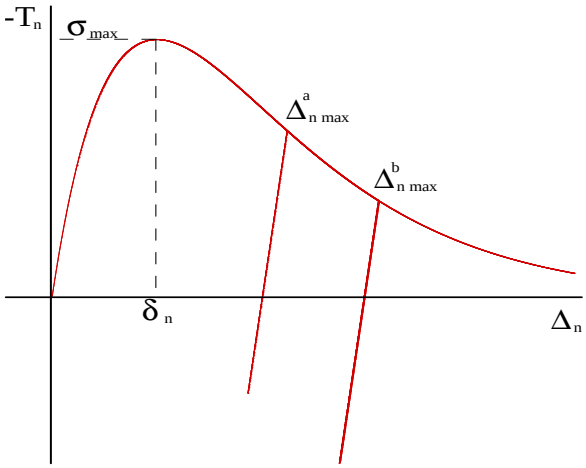

Figure 2: Irreversible cohesive law with residual opening.

Tangential traction (T_t) follows uniquely an exponential law (see Xu and Needleman, 1994), then no irreversibility is considered in this component.

3 FINITE ELEMENT IMPLEMENTATION

The rate of deformation [D] for the material can be written as (assuming small elastic rate of deformation):

$$[D] = [D^{e}] + [D^{pl}] \tag{5}$$

where $[D^{e}]$ is the elastic part and $[D^{pl}]$ is the plastic part of the rate of deformation. To calculate $[D^{pl}]$ a flow-rule/von Mises type constitutive law is used

$$[D^{pl}] = \Lambda [N] \tag{6}$$

where,

$$[N] = \frac{[\sigma']}{\sqrt{[\sigma'] \cdot [\sigma']}} \tag{7}$$

and

$$\Lambda = \frac{[N] \cdot [D]}{\left(1 + \frac{h}{3G}\right)} \tag{8}$$

$[\sigma']$ is the deviatoric stress, h is the hardening modulus and G is the shear modulus. σ_y is

updated using the evolution equation below:

$$\sigma_y = \sigma_y^0 + h\bar{\varepsilon}^{pl} \tag{9}$$

where σ_y^0 is the initial yield stress and $\bar{\varepsilon}^{pl}$ is the equivalent plastic strain. Objective stress rate $\left[\overset{\nabla}{\sigma}\right]$ is calculated as

$$\left[\overset{\nabla}{\sigma}\right] = [\Psi][D] \tag{10}$$

where $[\Psi]$ is the constitutive relationship that result from equations (6) to (9). Equation (10) together with co-rotational cohesive traction (equation 2), enable the use of the formulation in large displacements. The Principle of Virtual Work including cohesive traction, can be written as (with body and inertial forces neglected):

$$\int_\Omega [\sigma] : \left[\frac{\partial \delta U}{\partial X}\right] dV - \int_{\Gamma_f} \{F\}.\{\delta U\} dS + \int_{\Gamma_f} \{T\}.\{\delta \Delta\} dS = 0. \tag{11}$$

Bi-linear quadrilateral FE elements are used. The equation above is integrated in each FE volume Ω using one volumetric and four deviatoric Gauss points, where {U} are nodal displacements, {F} are prescribed forces on boundary Γ_f. Traction {T} is calculated in all FE faces using four Gauss points; integration is performed over the crack surface Γ_t. An implicit Newton-Raphson scheme is used to solve the corresponding equilibrium equations.

In the cases where inertial forces can not be neglected the explicit Central Differences Method is used to solve equilibrium equations.

4 NUMERICAL EXPERIMENTATION

Examples of application of the theory are divided in two parts. First it is shown the effect of cyclic loading on crack propagation (fatigue) in an aluminum specimen, neglecting inertial effects. Afterwards a case of impact, with monotonic loading is tested in order to verify the effect of unloading on crack propagation.

4.1 Fatigue test

The example modeled is a 7075-T6 aluminum specimen in plane strain. The aluminum is considered elasto-plastic with non-linear hardening by saturation. The properties are: longitudinal elastic modulus E=72000 MPa; poisson modulus ν=0.33; yielding stress σ_y =505 MPa; ultimate strength σ_u=570 MPa; ultimate strain ε_u=0,11.

To define the non-linear hardening by saturation (see equation 12) is necessary to define the constant η, that was adjusted to η=101,9 (this value makes that the ultimate strain ε_u occurs at the ultimate stress σ_u).

$$\sigma = \sigma_e + (\sigma_u - \sigma_e)[1 - \exp(-\eta \bar{\varepsilon}^{pl})] \tag{12}$$

where $\bar{\varepsilon}^{pl}$ is the equivalent plastic strain. The cohesive interface properties are defined as follows: fracture energy ϕ_n=7,74 N/mm; maximum normal traction: σ_{max}=3 x σ_y=1515 MPa; characteristic length: δ_n=1,88x10^{-3}mm. The geometry is described in Figure 3:

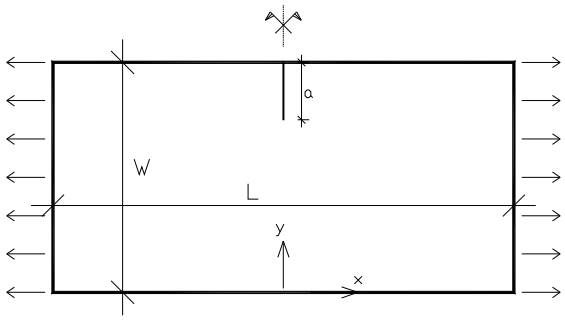

Figura 3. Specimen geometry (L=40 mm; W=20 mm; a=5 mm)

Half of the piece was modeled, using symmetry. The crack has a length a=W/4, located at x=0. Interface elements where placed only in a straight line in the crack direction, from the crack tip to the end of piece. 20.000 bi-linear quadrilateral FEs where used, with characteristic length of 0,1 mm at the crack zone. 150 interface elements were used. The piece was subjected to prescribed force in x=L/2 and x=-L/2, from y=0 to y=W. Analysis were done for different loading functions but always linear, according to Figure 4 (in the figure, loads appear converted in remote applied traction. It was admitted that applied traction is uniform and obtained dividing loads by area).

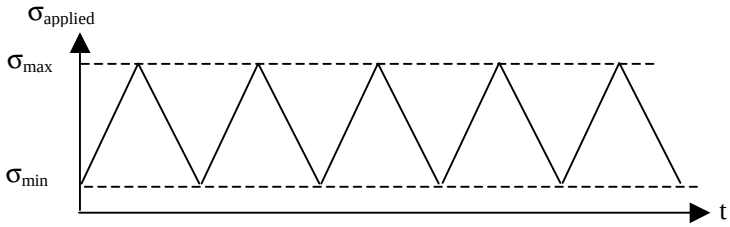

Figura 4. Cycles of loading and unloading.

In this case, the stress-intensity factor can be calculated as:

$$\Delta K_I = Y\Delta\sigma\sqrt{\pi a} = \underbrace{Y\sigma_{max}\sqrt{\pi a}}_{K_I^{max}} - \underbrace{Y\sigma_{min}\sqrt{\pi a}}_{K_I^{min}} \quad (13)$$

The interface is considered cracked for $\Delta_n \geq 5\delta_n$. The static force necessary for propagation is the force that produce a stress-intensity factor K_I equal to its critical value K_{IC}. Considering material data and using equation (14), K_{IC} can be calculated as 25 MPa.m$^{1/2}$.

$$K_{IC} = \sqrt{\frac{\phi_n . E}{(1-\nu^2)}} \quad (14)$$

The value of the stress-intensity factor K_I can be obtained by equation (13) (for the case in study, Ewalds e Wanhill, 1986, define the value of the geometric function Y). For $K_I=K_{IC}$, the theoretical force necessary to begin propagation is 2624 N. The numerical force obtained was 2626 N, which indicates that discretization was correct and the LEFM was valid.

The Table 1 below shows the results of propagation obtained in cyclic loading, for different values of ΔK, R and α. The value of α, used in equation (4), determines the declivity of unloading curve. The greater the α, the greater the declivity and a larger residual opening is obtained. Then a relationship of α with the thickness of oxide can be established: the greater the α, the greater the oxide layer.

R	0,0	0,0	0,0	0,111	0,111	0,167	0,222
ΔK_I	21,25	22,5	23,75	21,25	20,0	18,75	17,5
α	5,0	1,0	0,35	0,5	1,0	1	0,5
da/dN	0,01	0,022	0,029	0,029	0,013	0,007	0,01

Tabela 1: Crack propagation velocity (ΔK_I in $MPa\sqrt{m}$; da/dN in mm).

Points of Table 1 are plotted in Figure 5, together with experimental data. To obtain a better fitting with experiments, in general it is necessary to increase α with ΔK. Then the residual opening has the tendency to increase with the decrease of ΔK, which finds experimental background considering that for low ΔK a greater friction between crack faces occur, leading to greater oxide build up. The greater friction with low ΔK values occurs because crack is less opened and roughness is greater (see Figure 1).

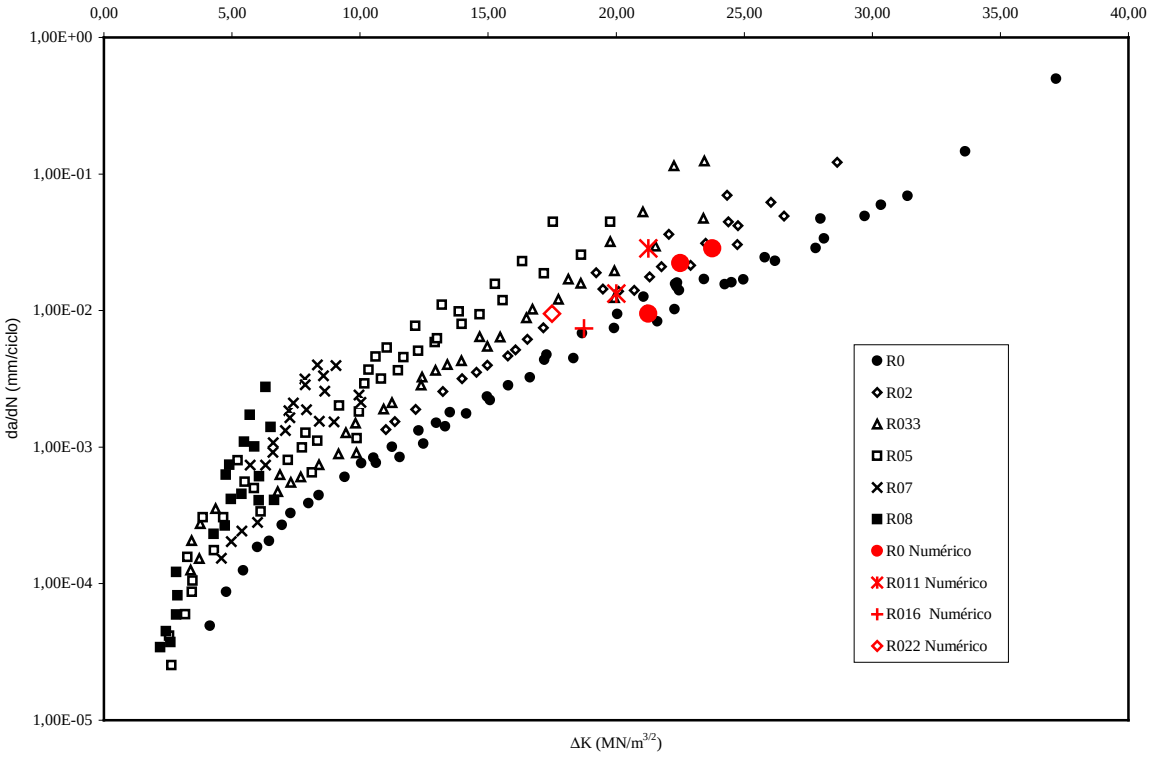

Figura 5. Experimental data [14] *x* numerical simulation (Al 7075-T6)

Figure 6 shows the relation α *x* ΔK for best data fitting. It is evident the described trend. Besides, for greater R (greater average stress), the layer of oxides necessary to fit numerical with experimental results has the tendency to be smaller due to smaller friction, which is evident in the figure 5.

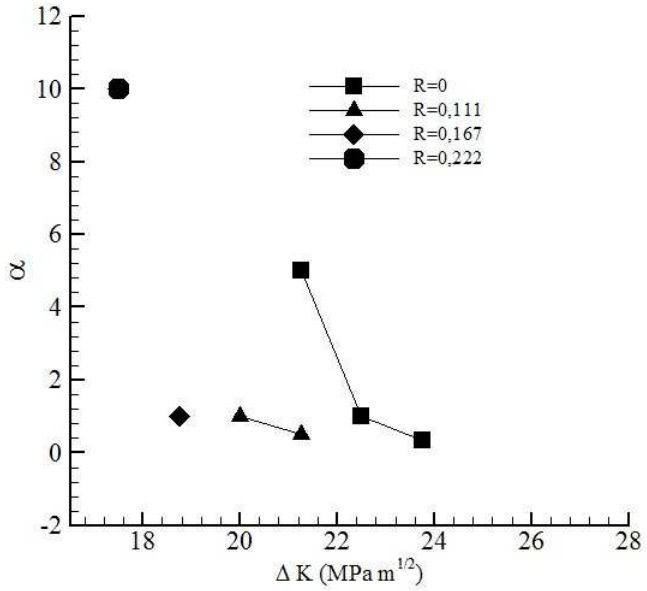

Figura 6. α values fitted for different values of ΔK and R.

4.2 Dynamic test

The example modeled consisted of a PMMA (Polimetacrilate of Metila) piece, in plane strain under dynamic loading. The material is considered elastic. The external loading is monotonic crescent, however local unloading may occur at the crack tip, as it will be shown as follows. The material properties are: elastic longitudinal modulus E=3240 MPa; poisson coefficient ν = 0.35; specific mass ρ = 1190 kg/m³; normal fracture energy ϕ_n=352.3 J/m²; tangential fracture energy ϕ_t=352.3 J/m²; maximum normal traction σ_{max}=E/10=324 MPa; maximum tangential traction τ_{max}=755.4 MPa; normal characteristic length δ_n=0.4 x 10^{-6} m; tangential characteristic length δ_t=0.4 x 10^{-6} m. The geometry is described in Figure 7.

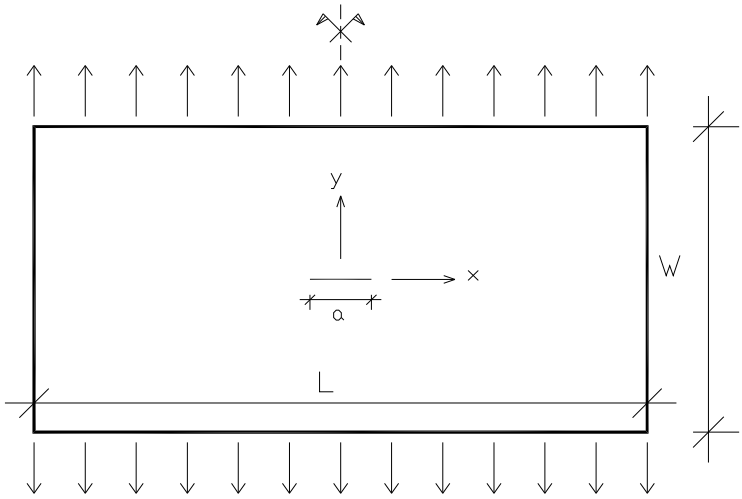

Figure 7: Specimen geometry (L=6 mm; W=3 mm; a=0.6 mm)

Half of the specimen was modeled due to symmetry. Interface cohesive elements were placed between all FEs (then, contrary to the previous example, the crack is free to propagate in all directions). 6400 volumetric FEs (quadrilaterals degenerated into triangles) and 9516

interface elements were employed. The characteristic FE dimension is 0.0375 mm. Displacement u_x=0 at x=0 from y=-W/2 to y=W/2. The other boundary conditions are defined by equations below:

$$u_y(t) = \int_0^t V_{ys}(t)dt \text{ in } y = \frac{W}{2} \tag{15}$$

$$u_y(t) = \int_0^t V_{yi}(t)dt \text{ in } y = -\frac{W}{2} \tag{16}$$

$$V_{ys} = \begin{cases} V_s t / t_r & \text{for} \quad t \le t_r \\ V_s & \text{for} \quad t > t_r \end{cases} \tag{17}$$

$$V_{yi} = \begin{cases} V_i t / t_r & \text{for} \quad t \le t_r \\ V_i & \text{for} \quad t > t_r \end{cases} \tag{18}$$

where V_s is the impact velocity at the superior boundary and V_i is the impact velocity at the inferior boundary. t_r=0.1 μs. Total analysis time is 10 μs. The interface is considered cracked for $\Delta_n \ge 5\delta_n$.

The explicit Central Differences Method was used to solve equilibrium equations. Theoretically maximum time increment (Δt_c) for the method (CFL condition, see, for instance, Hughes, 1990) is l_{min}/c_d where l_{min} is the minimal dimension of the FE and c_d is the velocity of pressure waves of the material. This critical time-step calculation will work out only if interface elements are not used. The problem introduced by interface elements is that l_{min} value tends to zero. Then the CFL loses its application here and a much smaller time step must be used in order to guarantee stability. In the case studied here a time-step around 200 times smaller than CFL condition (considering only standard FE) had to be used in order to guarantee stability.

Due to the absence of oxides and assuming a fragile rupture, unloading will occur to origin, or no residual opening is assumed. Figure 8 presents results of the simulation for two different situations: a) unloading following the original exponential relation (equation 3) and b) unloading following a linear relation (equation 4, α in this case is variable). It can be seen that, in case “a” a linear propagation occurs for 0.60 mm and then the crack bifurcates, while for case “b” propagation before bifurcation occurs for 0.75 mm. It can be concluded that a local unloading at the crack tip effectively took place, even for the monotonically crescent applied loading. Also, it can be concluded that a dissipation was introduced by the linear unloading, which permitted that crack propagated without bifurcation for a longer distance. Also the results presented in Figure 8b are coincident with results presented by Xu and Needleman (1994).

Different values of V_i and V_s were studied in Machado (2007). The trend described above was also found.

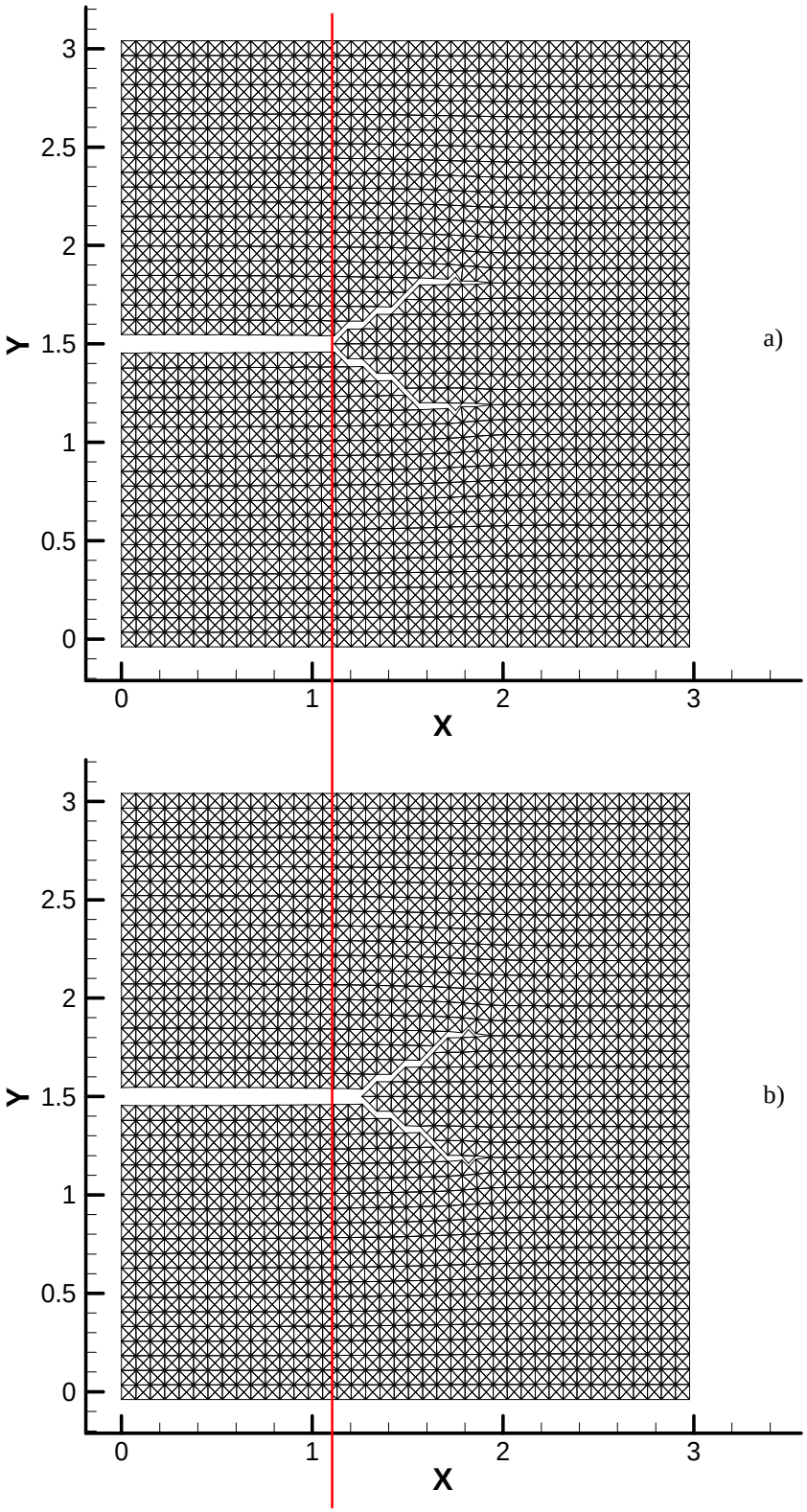

Figure 8: Propagation after 8.0 μs. V_s = 5 m/s and V_i = -5 m/s. a) exponential unloading; b) linear unloading. Vertical line indicates begin of bifurcation for case “a”.

5 CONCLUSIONS

Direct use of cohesive interface methodology, as originally proposed, is not able to model fatigue phenomenon correctly, unless some degree of irreversibility be introduced in the interface constitutive law. In this work, oxide formation after crack opening was considered the key factor leading to irreversibility. The oxide layer increases crack opening after each cycle. This effect can also be associated to contact between crack surface peaks and valleys.

The hypothesis leads to numerical results consistent with experiments, at least in the range studied:

- Relatively high values of ΔK ranging from 0,6 to 0,95 K_{IC}.
- Relatively small values of R ranging from 0 to 0,2.

To obtain a correct fitting with experiments, α had to be changed:

- For larger values of ΔK, smaller values of α had to be used. Physically this hypothesis means that a greater oxide layer is created for smaller values of ΔK.
- This trend decrease when R, or the average stress, increases.

Experimental evidences subsidize this behavior: For smaller values of ΔK the crack opening is smaller and superficial roughness is increased (Kamp et al., 2007). Friction between surfaces should increase in this case, leading to enhanced oxide formation (Suresh et al., 1981).

Besides oxide formation, a greater superficial roughness can lead to a greater residual opening due to peak/valley misfit caused by plastic deformation or other effect, after each cycle. Kamp et al. (2007) showed that misfit of crack surfaces may lead to early surface contact even for large values of ΔK.

The average value found here for the “m” exponent of Paris’ law (see equation 1), was approximately 4, which is in accordance with values reported in the literature (Nguyen et al., 2000 and Deshpande et al. 2002).

If only monotonically crescent loading is considered, it can be concluded that:

- Unloading of the cohesive law is important and can not be neglected.
- A linear path during unloading leads to energy dissipation, even when no residual opening is introduced. This dissipation was here shown by retardation of bifurcation in the impact of a fragile material.

As a byproduct of this research, it was concluded also that critical time-step used in the Central Difference Method, based on minimal FE size, can not be used when cohesive interface are embedded in a standard FE mesh.

ACKNOWLEDGEMENTS

To CNPq, Projeto Universal num. 473054/2003-5, by financial support.

REFERENCES

de-Andrés, A., Pérez, J.L and Ortiz, M., Elastoplastic finite element analysis of three-dimensional fatigue crack growth in aluminum shafts subjected to axial loading. *International Journal of Solids and Structures*, 36:2231-2258, 1999.

Deshpande, V.S., Needleman, A. and Van der Giessen, E., Discrete dislocation modeling of fatigue crack propagation. *Acta Materialia*, 50:831-846, 2002.

Do, T., Splinter, S.J., Chen, S. and McIntyre, N.S. The oxidation kinetics of Mg and A1 surfaces studied by AES and XPS. *Surface Science*, 387:192-198, 1997.

Edwalds, H.L. and Wanhill, R.J.H., *Fracture Mechanics*. Delftse Uitgevers Maatschapij,

1986.
Hudson, C.M., *Effect of stress ratio on fatigue-crack growth in 7075-T6 and 2024-T3 aluminum alloy specimens*. NASA TN D5390, 1969.
Hughes, T.J.R., *The finite element method – linear static and dynamic finite element analysis.* Prentice Hall, 1987.
Kamp, N., Gao, N., Starink, M.J., Parry, M.R., and Sinclair, I., Analytical modeling of the influence of local mixed mode displacements on roughness induced crack closure. *International Journal of Fatigue*, 29:897-908, 2007.
Machado, A. *Uso do método das interfaces coesivas na simulação do processo de propagação de trincas por fadiga.* MSc Thesis, PPGEC/UFRGS, 2007.
Needleman, A., A continuum model for void nucleation by inclusion debonding. *Journal of Applied Mechanics*, 54:525-531, 1987.
Nguyen, O., Repetto, E.A., Ortiz M. and Radovitzky, R.A., A cohesive model of fatigue crack growth. *International Journal of Fracture*, 110:351-369, 2001.
Peloux, R.M.N., Crack extension by alternating shear. *Engineering Fracture Mechanics*, 1:697-704, 1970.
Roe, K.L. and Sigmund, T.,An irreversible cohesive zone model for interface fatigue crack growth simulation. *Engineering Fracture Mechanics*, 70:209-232. 2003.
Suresh, S., *Fatigue of Materials*, Cambridge University Press, 1998.
Suresh, S., Zaminski, G.F. and Ritchie, R.O., Oxide induced crack closure: an explanation for near-threshold corrosion fatigue crack growth behavior. *Metallurgical Transactions*, 12^{A}:1435-1443, 1981
Ural, A., Krishnan, V.R., and Papoulia, K.D., A damage-based cohesive model for simulating fatigue crack growth; in preparation, 2007.
Xu, X.P. and Needleman, A.,Numerical simulation of crack growth in brittle solids. *Journal of the Mechanics and Physics of Solids*, 42:1397-1434, 1994.